2014 IEEE International Conference on Robotics & Automation (ICRA)
Hong Kong Convention and Exhibition Center
May 31 - June 7, 2014. Hong Kong, China

Experimental Characterization of Bowden Cable Friction

Dongyang Chen, Youngmok Yun and Ashish D. Deshpande

Abstract— **This paper presents a systematic method for experimental characterization of Bowden cable friction. A novel tension measurement method using a motion capture system and a spring is introduced. With the tension measurement method, the effects of nine variables on friction are investigated. Experimental results show that i) a combination of 7x19 FEP-coated stainless steel cable and double-sheaths has the highest force transmission efficiency; ii) smaller coefficient of friction material, smaller cable moving speed, shorter cable length, longer clamp distance, stiffer cable/sheath all help to increase the force transmission efficiency; and iii) the static friction pretension ratio only decreases as the coefficient of friction of cable/sheath decreases or as cable/sheath stiffness increases. We have generated guidelines for the Bowden cable performance which may help robotics researchers in choosing materials for the Bowden cables and designing control systems for actuation.**

I. Introduction

A Bowden cable is a type of flexible cable used to transmit mechanical force or energy by the movement of an inner cable relative to a hollow outer sheath. It has been widely used in complex and space-constrained environments, typically in car and bike brake systems. Recently, many robotic researchers, particularly those who design wearable robots and medical devices, have introduced Bowden cables into robot applications [1–6]. We also plan to use Bowden cable actuation in a novel hand exoskeleton [7].

Bowden cables have several advantages which make them attractive for robot applications. The first one is remote actuation. Many robot systems suffer from the mass/moment of inertia of actuators and transmission systems because they change the dynamic properties of the system. The mass/moment of inertia especially degrade the transparency of wearable robots. By using a Bowden cable, the actuators can be placed away from the end-effectors, which helps to reduce the weight and increase the power density. The second advantage is flexibility. Most of mechanical transmission systems such as gear trains, torsion bars and levers are rigid, which restricts the configuration and range of motion of the system. Since a Bowden cable is only clamped at the ends, it is a essentially a routing-free solution which makes it flexible. Third, the routing path of a Bowden cable can be freely changed without reaction forces while other transmission systems need reaction forces to change the path of transmission. For example, a cable driven system needs reaction forces from pulleys to change its routing path, which affects robot dynamics. And the location where reaction force is exerted on robot systems can be changed by using Bowden cables. In theory, Bowden cables can isolate load actuators without reaction forces, as will be described in later section.

However, a critical weakness of a Bowden cable is the high friction, which is generated between the inner cable and outer sheath and degrades the performance of the transmission system. [8] report that their robot consumes 90% of the energy to overcome the friction. Despite the significant influence of the friction, most robot researchers have regarded it as a disturbance in their control scheme [2][9][10] because it is hard to compensate for it due to its non-linearity and multi-variable dependency.

There have been a limited number of studies on Bowden cable friction. Lawrence et al. [11] used a simple model to express the force relationships at both extremities of a Bowden cable, which only considered the coefficient of friction and wrapping angle as influencing factors. Goiriena et al. [12] only partially showed the influence of some variables on friction using only steel cables and one sheath. There is no systematic method for characterizing the performance of Bowden cables, leading to difficulty in the selection of proper Bowden cables and in designing control systems for Bowden cable actuated robots.

This paper presents a systematic experimental method for the characterization of friction for small-sized Bowden cable systems. Since friction depends on many variables including material properties, length, configuration etc, we choose not to develop a theoretical model. The paper first introduces a friction measurement method with a novel tension measurement technique using a motion capture system and springs. Second, the best combination of inner cable and outer sheath is determined after exploring fifteen different candidates through comprehensive experiments. Finally the influence of a number of variables including cable speed, pretension, cable length, clamp distance and clamp orientation on friction is investigated.

Our study may help robotics researchers in design of hardware and controller. The selection of actuator size is an important design decision and the estimation of external disturbance influences controls greatly. We provide guidelines for the selection of Bowden cable configurations, and the range of friction for the given condition based on the experimental analysis.

This work was supported, in part, by the National Science Foundation (NSF) grant #NSF-CPS-1135949.

D. Chen and Y. Yun are graduate students of Mechanical Engineering, The University of Texas at Austin, 3.130, ETC, Austin, Texas, USA (dongyangchen, yunyoungmok)@utexas.edu

A.D. Deshpande is a faculty of Mechanical Engineering, The University of Texas at Austin, 3.130, ETC, Austin, Texas, USA (ashish@austin.utexas.edu)

978-1-4799-3684-7/14/$31.00 ©2014 IEEE

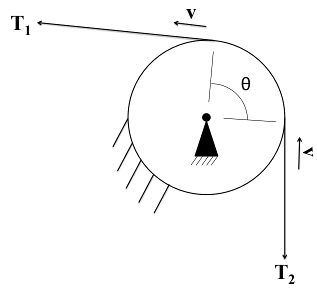

Fig. 1: Illustration of Capstan formula. The interaction between a cable and sheath is assumed to be similar to a rope routed and sliding around a stationary sheave at a constant speed. θ is the wrapping angle, T_1 is the input force and T_2 is the output force.

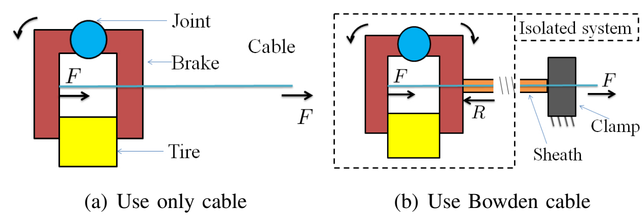

Fig. 2: Illustration of a Bowden cable used in a brake system. By using a Bowden cable, the reaction force generated by the sheath counteracts the external force and helps to isolate the system.

II. Experiment Design

A. Theoretical Background

So far the only theoretical model for describing Bowden cable friction is the Capstan formula [11, 12] as follows:

$$T_1 = T_2 e^{\mu\theta} \tag{1}$$

where μ is the kinetic coefficient of friction between the cable and sheath, θ is the total wrapping angle, T_1 is the input force and T_2 is the output force (Fig. 1). Numerous factors affect the performance of a Bowden cable, but this model only considers two factors μ and θ. Hence it is limited in describing the actual behaviour. Given the complexity of friction behaviour, we propose to characterize Bowden cable friction through experiments.

The buckling effect of Bowden cables is also an important factor for studying friction. Fig. 2 shows a typical bike brake system. For situation (a), it only uses a cable, and thus the whole structure tends to move to the right when the external force is applied on the cable because there is no reaction force to counteract the external force. However when a Bowden cable is used as in situation (b), since the sheath is clamped at both ends, it will apply a reaction force to the structure and make it isolated. This is one of the advantages of Bowden cables as mentioned in Introduction. However this brings forth the buckling problem, which causes the deformation of the sheath and makes the other influencing factors, especially the wrapping angle, indeterministic. To account for such effects, we include the stiffness of cables and sheaths as variables for our experiments.

B. Experiment Methodology

1) Variables selection and experiment procedure: The friction of a Bowden cable is determined by measuring the difference in tension before and after the Bowden cable. Instead of using a force sensor, we propose a novel tension measurement method using a motion capture system and springs. This new method is described and evaluated in Section III.

Among the possible factors influencing static and kinetic friction, we chose and investigated nine variables for our experiment: stiffness of cable and sheath, material of cable and sheath, cable length, clamp orientation, clamp distance, pretension and cable speed. To reduce the number of unnecessary experiments, we divided the experiments into two steps. First we determined the optimal combination of cable and sheath, which will be shown in Section IV. Then in Section V, we investigated the influences of other variables on friction by experimenting with the best combinations of cable and sheath as determined in the previous step.

2) Evaluation Criteria: In this paper, we use force transmission efficiency defined by (2) and static friction pretension ratio defined by (3) as the criteria to compare experimental results of different cases. The force transmission efficiency is equal to the quotient of the tension in the cable after the sheath, T_2 divided by that before the sheath, T_1. And the static friction pretension ratio is equal to the quotient of the maximum static friction, f_{SM} divided by the pretension in the cable after the sheath, T_2^0. The force transmission efficiency reflects kinetic friction, while the static friction pretension ratio reflects static friction. High force transmission efficiency and low static friction pretension ratio is desired in a Bowden cable system.

$$R_k = T_2 \ / \ T_1 \tag{2}$$

$$R_s = f_{SM} \ / \ T_2^0 \tag{3}$$

Except for the stiffness and material type of cable and sheath, all the other variables have little effect on static friction pretension ratio. Therefore, only in the stiffness and material sections of Section IV, the effects on static friction pretension ratio will be discussed. And the maximum static friction is used to evaluate the effect of pretension because it is the only factor influenced by pretension.

III. Calibration and Verification of Force Measurement System

The usual way to measure force or tension is to use a load cell or force gauge. However the main drawback of a force sensor is that its weight is usually not negligible for the original system. The inclusion of the mass may change the dynamic characteristics of the system and in turn affect the force measurement accuracy.

We introduce a new way of force measurement using a motion capture system (PhaseSpace Inc.) with springs. The idea is to attach markers to both ends of a spring, and insert the spring at any point where force is to be measured as shown in Fig. 3(a). Eight cameras are hung around the markers to capture the 3D motion of each marker. The deflection of the spring is recorded by the motion capture system, and the force is calculated using spring constant.

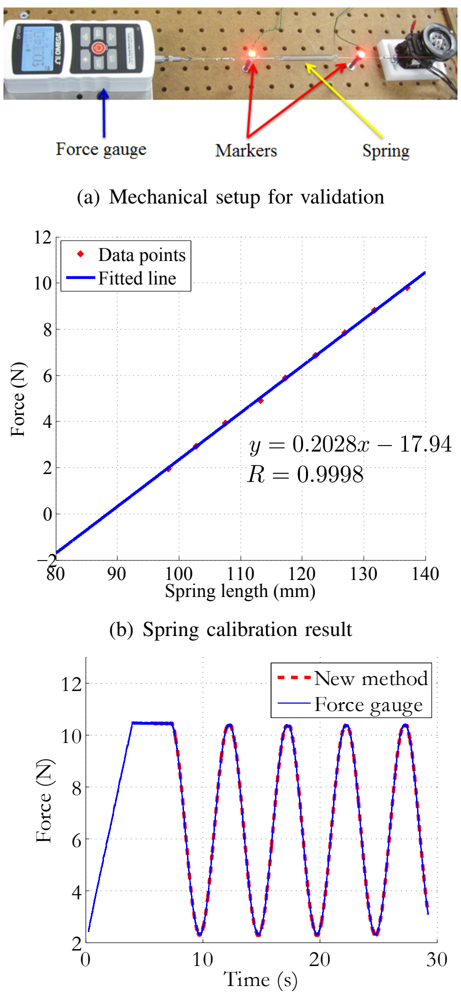

(a) Mechanical setup for validation

(b) Spring calibration result

(c) Force data comparison

Fig. 3: Validation of the new force measurement method. (a) The servo motor (Dynamixel RX-24F, ROBOTIS. Inc.) provides a sinusoidal force and the force is measured both by using a digital force gauge (DFG55, OMEGA. Inc.) and the novel measurement method. (b) The force measurement system is calibrated using a set of weights. The fitted line has a correlation coefficient of 0.9998 which shows the spring calibrated has linear behaviour. (c) The force measured by the new method and the force gauge are compared, the average error between the two sets of data is 0.01 N.

Since the mass of a spring is usually small, it has little effect on the dynamics of the original system.

To validate the performance of the novel tension measurement system, we first calibrated the spring and the experimental results show that the chosen spring has linear behaviour (Fig. 3(b)). Then we connected a motor, a string with the calibrated spring in series with a force gauge (Fig. 3(a)). We applied a sinusoidal force with a motor and measured it with both methods. The sampling rate of the force gauge is at 1000 Hz, while the new measurement system runs at 480 Hz. Results show that the novel force measurement method is accurate in a dynamic setting. The two curves in Fig. 3(c) are almost the same except for some data noises and the average error between the data from these two methods is around 0.01 N.

IV. Determination of the Best Combination of Cable and Sheath

A. Experiment Methodology

There are many possibilities for cables and sheaths and selecting the right type of cable and sheath is crucial for all Bowden cable applications. Cables and sheaths can both be specified in terms of three major factors, namely stiffness, material and diameter. Generally the diameter of cables and sheaths is restricted by the application requirement such as load or size. Therefore, we focus on studying the influence of stiffness and material of cables and sheaths. For consistency, all the different types of cables we used have the same outer diameter of 0.635 mm, while all the sheaths have the same inner diameter of 1.016 mm.

According to the factors mentioned above, we used three types of sheaths for our experiment, Nylon sheath, PTFE (Polytetrafluoroethene) sheath and double-sheaths. The double-sheaths is made by inserting a PTFE sheath into an MFA (modified fluoroalkoxy) sheath and it becomes stiffer than a single PTFE sheath, while its inner material remains the same. Therefore, by comparing the experimental results of Nylon and PTFE sheaths, the effect of sheath material can be understood and by comparing the results of PTFE and double-sheaths, we can determine the effect of sheath stiffness.

We used five types of cables for our experiment, 1x7, 7x3 and 7x19 stainless steel cables, 7x19 Nylon-coated and 7x19 FEP (Fluorinated ethylene propylene)-coated cables. The stiffness of a cable is determined by the number of its strands and wires per strand (Fig. 4), which is indicated by their name (For example, a 7x19 cable consists of seven strand, each made with nineteen wires). And for the cables we used, 1x7 cables are the most stiff ones, while 7x19 cables are the most compliant ones, and the stiffness of 7x3 cables falls in between. Therefore, by comparing the experimental results of 1x7, 7x3 and 7x19 stainless cables, the effect of cable stiffness can be seen and by comparing the results of 7x19 stainless steel, 7x19 Nylon-coated and 7x19 FEP-coated cables, we can determine the the effect of cable materials.

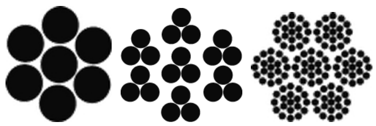

(a) 1x7 (b) 7x3 (c) 7x19

Fig. 4: Cable construction types (Pictures from McMaster.com). The name of a cable indicates its construction, for example an 1x7 cable consists of one strand, each made with seven wires. The construction mainly determines the stiffness of a cable. 1x7 cables have the largest stiffness, 7x19 cables have the smallest stiffness, and the stiffness of 7x3 cables falls in between.

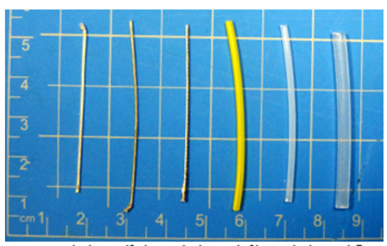

(a) (b) (c) (d) (e) (f)

Fig. 5: Cables and sheaths. (a) 7x19 FEP-coated cable; (b) 7x19 Nylon-coated cable; (c) Stainless steel cable; (d) Nylon sheath; (e) PTFE sheath; (f) MFA tube

TABLE I: Variables selected for the experiments. There are nine variables in total, including the stiffness of cable and sheath, material of cable and sheath, pretension, cable speed and geometrical factors such as cable length, clamp distance and clamp orientation. The different values used for each variable are shown in the table.

Cable	Stiffness	1x7/ 7x3/ 7x19
	Material	Stainless Steel/ Nylon-coated/ FEP-coated
Sheath	Stiffness	Single/ Double
	Material	Nylon/ PTFE
Geometry	Cable length(mm)	200/ 400/ 600
	Clamp orientation	45°/ 90°/ 180°
	Clamp distance(mm)	200/ 400/ 600
Pretension		Small/ Medium/ Large
Cable Speed(m/s)		0.023 / 0.046/ 0.069

In summary, we study three kinds of sheaths and five kinds of cables in all. Fig. 5 and Table I show all the cables and sheaths used in our experiments. Based on the number of types of cables and sheaths, there are fifteen different combinations in total. For all combinations, three different speeds and three different pretensions are tested. All the geometrical variables are controlled and maintained the same – 90° clamp orientation θ, 400 mm cable length l, 400 mm clamp distance d, as shown in Fig. 6.

In our experiment, we use a servo motor to load and unload the cables (Fig. 6). The motor first runs at three different speeds but starts from the same initial position so that we can check the effect of cable speed on friction, then it runs at a constant speed but with three different initial positions so that the effect of pretension on friction can be checked. And under every situation, the experiment is conducted for three times and the results are averaged.

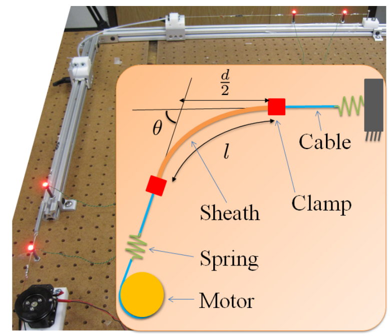

Fig. 6: Experiment setup. A motor is used to load and unload the cable, two springs attached with markers are used to measure the tension before and after the sheath. d is the clamp distance, l is the cable length, θ is the clamp orientation.

After the experiments, the tensions in the cables are calculated, and the output force T_2 is plotted versus the input force T_1. Fig. 7 shows a representative plot for one experiment. The curve can be divided into 6 segments and their meaning is:

1) A-B: This segment corresponds to the initial stationery phase of one cycle. The coordinates of point A reflect the pretension in the cables before and after the sheath. From point A to B, T_1 increases but T_2 remains the same, which means the cable has not started moving yet and point B is the moment when the maximum static friction is reached, thus the static friction pretension ratio is calculated at this point.

2) B-C: This segment corresponds to the forward static-to-kinetic transition phase. The difference between T_1 and T_2 becomes larger than the maximum static friction, and the cable starts moving. Because it takes some time for the cable to reach the predetermined constant speed from zero, the transition segment has some curvature.

3) C-D: This segment corresponds to the forward stable phase. The slope of this segment is the forward force transmission efficiency.

4) D-E: This segment corresponds to the forward kinetic-to-static transition phase. Because the motor stops much faster than the cable, the cable is still moving forward with a decreasing speed and T_2 increases while T_1 decreases till the cable stops moving.

5) E-H: These segments are the same phases as the ones stated before, the only difference is the direction of friction is changed.

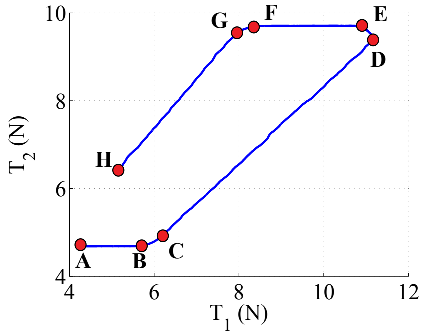

Fig. 7: A typical plot from an experiment with 1x7 stainless steel cable and PTFE sheath. From point A to point E is the loading period, while from F to H is the unloading period.

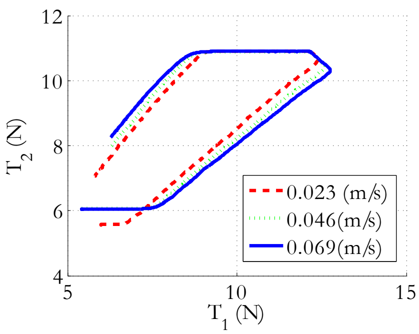

(a) The effect of cable speed on friction

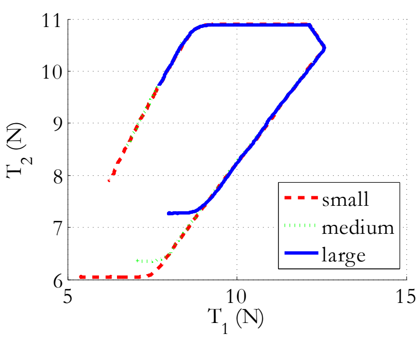

(b) The effect of pretension on friction

Fig. 8: Effects of cable speed and pretension on friction. (a) The slope of the forward stable segment, which corresponds to the force transmission efficiency, decreases as the cable speed increases. (b) The slope of the forward stable phase remains the same as pretension varies. Therefore the force transmission efficiency is not affected by pretension.

B. Results and Discussion

1) Cable speed: The larger the cable speed is, the less the force transmission efficiency is. Fig. 8(a) shows the effects of various cable speeds. As can be seen, the slope of the forward stable segment, which is the force transmission efficiency, decreases as speed increases. Same conclusions can be drawn by looking at Table II, for all different combinations of cables and sheaths, the efficiency decreases as speed increases. One reason for this is that Bowden cable friction includes some viscous friction. Another reason is that the coefficients of friction of the materials may increase with velocity.

2) Pretension: The larger the pretension is, the larger the maximum static friction is, but the force transmission efficiency remains the same. As can be seen in Fig. 8(b), the slopes of the forward stable segments are the same for all three pretensions, i.e. the efficiency is the same. This can be further observed by looking at Table II, where the efficiency values are very close to each other for the three different pretensions in all cases.

On the other hand, according to Fig. 8(b) and Table III, the increase in the pretension leads to the increase of the maximum static friction. The reason for this is that the increased pretension results in larger normal forces between the cable and sheath, and thus the maximum static friction

TABLE II: Force transmission efficiencies for the experiments to determine the best combination of cable and sheath. For the same kinds of sheath, stiffer cables and those with smaller coefficient of friction have larger force transmission efficiency. For the same kinds of cables, stiffer sheath and those with smaller coefficient of friction have larger force transmission efficiency. The efficiency decreases as cable speed increases, and it does not change as pretension varies. (S means small pretension, M means medium pretension and L means large pretension.)

PTFE		**Stainless Steel**			**Nylon**	**FEP**
		1x7	**7x3**	**7x19**	**7x19**	**7x19**
Cable Speed	**0.023 m/s**	0.834	0.797	0.764	0.849	0.894
	0.046 m/s	0.850	0.757	0.748	0.808	0.856
	0.069 m/s	0.849	0.741	0.740	0.789	0.826
Pretension	**S**	0.848	0.759	0.745	0.804	0.858
	M	0.853	0.751	0.750	0.794	0.852
	L	0.860	0.733	0.740	0.780	0.863

Nylon		**Stainless Steel**			**Nylon**	**FEP**
		1x7	**7x3**	**7x19**	**7x19**	**7x19**
Cable Speed	**0.023 m/s**	0.742	0.695	0.605	0.755	0.750
	0.046 m/s	0.729	0.668	0.590	0.716	0.715
	0.069 m/s	0.717	0.650	0.573	0.710	0.709
Pretension	**S**	0.721	0.661	0.581	0.722	0.722
	M	0.723	0.666	0.577	0.726	0.724
	L	0.694	0.673	0.597	0.743	0.722

Double-sheaths		**Stainless Steel**			**Nylon**	**FEP**
		1x7	**7x3**	**7x19**	**7x19**	**7x19**
Cable Speed	**0.023 m/s**	0.881	0.864	0.848	0.891	0.906
	0.046 m/s	0.897	0.870	0.845	0.874	0.891
	0.069 m/s	0.895	0.856	0.837	0.860	0.882
Pretension	**S**	0.889	0.856	0.839	0.875	0.896
	M	0.891	0.859	0.837	0.878	0.894
	L	0.891	0.869	0.821	0.879	0.901

increases. Note that we can not compare the values of the maximum static friction among different combinations because their pretensions are not controlled to be same.

3) Sheath and cable stiffness: The larger the sheath stiffness is, the larger the force transmission efficiency is. As can be seen in Table II, when paired with all kinds of cables, double-sheaths always has higher efficiency than the single PTFE sheath. For 7x3 and 7x19 stainless steel cables, the efficiency is increased by 10 percent when using a double-sheath instead of a single sheath. This is because under the same compressive force, a stiffer sheath has smaller deformation and wrapping angle than a compliant sheath, which results in higher efficiency according to the Capstan formula (1) and the experimental results of clamp orientation (Table VI(a)) shown in Section V. Cable stiffness has the same effect on force transmission efficiency as sheath stiffness does. As shown in Table II, 1x7 cable has the best performance among all stainless steel cables in all situations.

As regard to the static friction pretension ratio (Table IV), the increase of cable stiffness helps to lower the ratio and improves the Bowden cable performance. However, by comparing the results of PTFE sheath and double-sheaths, it can be seen that there is only small change in the ratio as sheath stiffness varies.

4) Sheath and cable material: The smaller the coefficient of friction between the sheath and cable is, the larger the force transmission efficiency and the smaller the static friction pretension ratio is. As shown in Table V, in terms of sheath material, PTFE has smaller coefficients of friction than Nylon for all cases. And for cable materials, FEP has the smallest coefficient of friction. This is consistent with our experimental results (Table II), i.e. PTFE sheath has larger efficiency than Nylon ones and FEP-coated cables have the largest efficiency.

There is one case where the coefficient of friction shows different results than the experiment results. When paired with PTFE sheath, Nylon cables are supposed to have larger coefficient of friction than stainless steel ones, however in Table II, 7x19 Nylon cables have larger efficiency than 7x19 stainless steel cables. The possible reason for this is that the coefficient of friction given in Table V is under the premise that the surface of both materials is smooth. However since the stainless steel cable is braided with multiple strands, the surface of the cable is relatively rough, which results in less efficiency.

Our results show that, overall the best combination from force transmission efficiency and static friction pretension ratio standpoints is 7x19 FEP-coated cable and double-sheaths.

V. Investigation of Effects of Geometrical Variables

A. Experiment Methodology

Here we study the effects of geometrical variables, as shown in Fig. 6, where l is the cable length, θ is the clamp orientation and d is the clamp distance. For the sake of space, we present results from experiments with only the best combination of cable and sheath: 7x19 FEP-coated cables and double-sheaths.

To determine the effects of clamp orientation, we ran the experiments at three different orientations (45°, 90°, 180°) with the following conditions: 400 mm cable length, 400 mm clamp distance, 0.046 m/s cable speed. To determine

TABLE III: Effect of pretension on the maximum static friction. The maximum static friction increases as the pretension increases. (S means small pretension, M means medium pretension and L means large pretension.)

		Stainless Steel			Nylon	FEP
		1x7	7x3	7x19	7x19	7x19
PTFE	S	1.274	1.388	1.414	1.243	1.149
	M	1.478	1.483	1.564	1.329	1.177
	L	1.647	1.717	1.874	1.407	1.198
Nylon	S	2.502	3.765	4.725	2.972	2.997
	M	2.760	3.879	4.759	3.260	3.316
	L	3.124	4.804	5.534	3.707	3.693
Double sheath	S	1.536	1.232	1.260	0.991	0.984
	M	1.573	1.434	1.438	1.155	1.139
	L	1.734	1.540	1.520	1.252	1.163

TABLE IV: Static friction pretension ratios for the experiments to determine the best combiantion of cable and sheath. Other factors except for cable and sheath, do not have significant effect on static friction pretension ratio. The ratio decreases as the stiffness of cable and sheath increases and smaller coefficient of friction also helps to reduce the ratio, which means better performance.

	Stainless Steel			Nylon	FEP
	1x7	7x3	7x19	7x19	7x19
PTFE	0.250	0.277	0.308	0.247	0.183
Nylon	0.557	0.611	0.753	0.688	0.652
Double sheaths	0.246	0.267	0.300	0.221	0.211

TABLE V: Coefficient of friction of different material pairs (from McMaster.com).

		Cables		
		Stainless Steel	Nylon	FEP
Sheath	Nylon	0.35	0.15 - 0.25	0.2
	PTFE	0.04	0.2	0.04

TABLE VI: Effects of geometrical variables on force transmission efficiency. (a) 400 mm cable length, 400 mm clamp distance and 0.046 m/s cable speed (b) 200 mm clamp distance, 90° clamp orientation and 0.046 m/s cable speed (c) 600 mm cable length, 90° clamp orientation and 0.046 m/s cable speed

(a) Clamp orientation			(b) Cable length(mm)			(c) Clamp dist.(mm)		
45°	90°	180°	200	400	600	200	400	600
0.809	0.766	0.673	0.800	0.723	0.690	0.728	0.746	0.776

the effects of cable length, we ran the experiments with three different lengths (200 mm, 400 mm, 600 mm) with the following conditions: 200 mm clamp distance, 90° clamp orientation and 0.046 m/s cable speed. To determine the effects of clamp distance, we ran the experiments with three different distances (200 mm, 400 mm, 600 mm) with the following conditions: 600 mm cable length, 90° clamp orientation and 0.046 m/s cable speed.

B. Results and Discussion

1) Clamp orientation: The larger the clamp orientation angle θ is, the lower the force transmission efficiency is. As shown in Table VI, as θ increases, the efficiency drops from about 80 percent to 67 percent. This is consistent with the Capstan model, because the total wrapping angle of the cable around the sheath increases as θ increases.

2) Clamp distance and cable length: The longer the cable and the shorter the clamp distance is, the lower the force transmission efficiency is. For the same clamp distance, the efficiency drops as cable length increases (Table VI). And for the same cable length, the efficiency drops as clamp distance decreases (Table VI). This is because when the clamp distance decreases or the cable length increases, larger and larger part of the cable will lose the constraint from the clamps which leads to the increase in wrapping angle and even buckling.

VI. Limitation and Conclusion

One limitation of the study is that there may be potential correlations among the nine factors which was not investigated. Another limitation is that Bowden cables are not only used for force transmission but for motion transmission in some cases as well. The elongation and deformation of Bowden cables should be considered when controlling positions. These limitations are part of future work. Finally, this paper only studies the characteristics of small Bowden cables. While they are smaller than bike cables, they are often used in robotic applications. The experimental results show that the characteristics of small Bowden cables may hold for larger ones as well.

We present a systematic experimental method for the characterization of Bowden cable friction. We have introduced a novel force measurement method based on a motion capture system and a spring and have validated its performance. Through the comprehensive experiments results, the best combination of cable and sheath having the highest force transmission efficiency is determined, which is: 7x19 FEP-coated cable and double-sheaths. We have investigated the effects of nine variables, including material and stiffness of cables and sheaths, cable speed, pretension, clamp distance, clamp orientation and cable length on the force transmission efficiency and static friction pretension ratio. We have generated guidelines for the Bowden cable performance, and depending on the need of their applications, robotics researchers could benefit from these results when choosing Bowden cables and designing control systems.

Acknowledgment

This work was supported, in part, by the National Science Foundation (NSF) grant #NSF-CPS-1135949. The contents are solely the responsibility of the authors and do not necessarily represent the official views of the NSF. The authors thank Prashant Rao and Priyanshu Agarwal for assisting in data acquisition setup.

References

[1] A. Schiele, P. Letier, R. van der Linde, and F. van der Helm, "Bowden cable actuator for force-feedback exoskeletons," in *IEEE/RSJ International Conference on Intelligent Robots and Systems*, pp. 3599–3604, 2006.

[2] H. Vallery, J. Veneman, E. van Asseldonk, R. Ekkelenkamp, M. Buss, and H. van Der Kooij, "Compliant actuation of rehabilitation robots," *Robotics Automation Magazine, IEEE*, vol. 15, no. 3, pp. 60–69, 2008.

[3] J. S. Sulzer, R. A. Roiz, M. A. Peshkin, and J. L. Patton, "A highly backdrivable, lightweight knee actuator for investigating gait in stroke," *Robotics, IEEE Transactions on*, vol. 25, no. 3, pp. 539–548, 2009.

[4] M. Braun, "Surgical instrument with elastically movable instrument head," Oct. 18 2012. US Patent 20,120,265,176.

[5] Q. Wu and X. Wang, "Design of a gravity balanced upper limb exoskeleton with bowden cable actuators," in *Mechatronic Systems*, no. 1, pp. 678–683, 2013.

[6] B. Weitzner, J. Golden, R. Rothstein, A. Chen, D. Bacon, K. Dang, *et al.*, "Medical device control system," Nov. 15 2011. US Patent 8,057,462.

[7] P. Agarwal, J. Fox, Y. Yun, D. Chen, M. K. OMalley, and A. D. Deshpande, "A novel index-finger exoskeleton with series elastic actuation: Design and kinematic characterization," in *IEEE International Conference on Robotics and Automation*, under review, 2014.

[8] J. Li, R. Zheng, Y. Zhang, and J. Yao, "iHandRehab: An interactive hand exoskeleton for active and passive rehabilitation," in *IEEE International Conference on Rehabilitation Robotics (ICORR)*, pp. 1–6, 2011.

[9] P. Letier, A. Schiele, M. Avraam, M. Horodinca, and A. Preumont, "Bowden cable actuator for torque-feedback in haptic applications," in *Proc. Eurohaptics 2006 Conf., Paris, July 2006*, 2006.

[10] A. Schiele, P. Letier, R. Van Der Linde, and F. Van Der Helm, "Bowden cable actuator for force-feedback exoskeletons," in *Intelligent Robots and Systems, 2006 IEEE/RSJ International Conference on*, pp. 3599–3604, IEEE, 2006.

[11] L. E. Carlson, B. D. Veatch, and D. D. Frey, "Efficiency of prosthetic cable and housing," *Journal of Prosthetics and Orthotics*, vol. 7, no. 3, pp. 96–99, 1995.

[12] A. Goiriena, I. Retolaza, A. Cenitagoya, F. Martinez, S. Riano, and J. Landaluze, "Analysis of bowden cable transmission performance for orthosis applications," in *IEEE International Conference on Mechatronics*, pp. 1–6, 2009.